FACULDADE DE MEDICINA DA UNIVERSIDADE DE COIMBRA

MESTRADO INTEGRADO EM MEDICINA – TRABALHO FINAL

CARLOS FERNANDO DIAS RODRIGUES

Stromal cells-derived IL-6, G-CSF and Activin-A induce dedifferentiation of lung carcinoma cells into cancer stem cells

ARTIGO CIENTÍFICO ORIGINAL

ÁREA CIENTÍFICA DE BIOLOGIA CELULAR

Trabalho realizado sob a orientação de:

MARIA CARMEN MARTINS DE CARVALHO ALPOIM

MARÇO/2017

Stromal cells-derived IL-6, G-CSF and Activin-A induce dedifferentiation of lung carcinoma cells into cancer stem cells

Carlos F. D. Rodrigues

Faculdade de Medicina
Universidade de Coimbra

Dissertação submitida à FMUC de acordo com o requerido
para a candidatura à obtenção do grau de

Mestre em Medicina
Área Científica de Biologia Celular

Coimbra, Março 2017

rodriguescfd@gmail.com

Publicado em Portugal em Março de 2017

Aos meus pais.

“Recomeça...

Se puderes,
Sem angústia e sem pressa.
E os passos que deres,
Nesse caminho duro do futuro,
Dá-os em liberdade.
Enquanto não alcances
Não descanses.
De nenhum fruto queiras só metade.

E, nunca saciado,
Vai colhendo
Ilusões sucessivas no pomar
Sempre a sonhar
E vendo,
Acordado,
O logro da aventura.
És homem, não te esqueças!
Só é tua loucura
Onde, com lucidez, te reconheças.”

Miguel Torga

O presente trabalho foi realizado no Centro de Neurociências e Biologia Celular da Universidade de Coimbra, Coimbra, Portugal, sob a orientação científica da Prof. Dra. Maria Carmen Alpoim. Trata-se de um trabalho de equipa que resultou num manuscrito submetido para publicação na revista *Proceedings of the National Academy of Sciences*.

O projeto no qual este trabalho se encontra inserido foi suportado por uma bolsa de investigação atribuída pela Fundação para a Ciência e Tecnologia a Maria Carmen Alpoim (PTDC/BBB-BQB/2450/2012), outra bolsa de investigação, atribuída pela mesma instituição, a Rui Pinto Pedrosa (PTDC/MAR-BIO/6149/2014) e ainda por uma bolsa de projeto financiada pelo Centro de Investigação em Meio Ambiente, Genética e Oncobiologia (CIMAGO) da FMUC (Projeto 16/06), também atribuída a Maria Carmen Alpoim.

Abstract

Cancer stem cells (CSCs) are a small population of extremely resistant cells inhabiting the tumors. Although comprising only as much as 3 % of the total tumor mass, these cellular population was demonstrated to orchestrate tumorigenesis and differentiation, underlying tumors' heterogeneity and mediating chemo- and radiotherapy resistance, and tumor relapse. Some authors even propose these cells as the drivers of the metastatic disease. Here we show that, as previous literature suggested, CSCs may actually be formed by dedifferentiation of terminally differentiated tumor cells, under stress conditions. In our system, nutrients and oxygen deprivation when tumor cells were injected in the subcutaneous space of immunocompromised mice was enough to activate non-malignant mice stromal fibroblasts, which established with tumor cells a paracrine loop mediated by Interleukine-6 (IL-6), Activin-A and Granulocyte colony-stimulating factor (G-CSF), thus regulating subsequent tumor formation and cellular differentiation. Moreover, we were able to dissect that cytokines were being released inside exosomes and that by scavenging the cytokines from the media and/or blocking exosomes' release, the dedifferentiation process was abrogated. Hence, it is the first time the exosomes are implicated in the dedifferentiation of CSCs, which opens new avenues of research regarding their potential use in targeted cancer therapies.

Significance

Understanding the process of cancer formation has long been a major and very active focus of research. The relatively recent discovery of cancer stem cells and the dissection of their biological traits lead to the hypothesis that through the targeting of this particular cellular population, the carcinogenic process may be abrogated, as may tumor progression to metastatic disease. Our report shows that cancer stem cells can be formed by stoma-orchestrated dedifferentiation of tumor cells through a paracrine communication mediated by exosomes. Altogether, the attained results identified IL-6 and Activin-A as the drivers of dedifferentiation and suggested their direct blockage and/or the blockage of exosomes' release as potential therapeutic strategies against cancer progression, with potential impact on clinical practice.

Resumo

As células estaminais tumorais (CETs) são uma fração extremamente resistente de células tumorais. Embora representem apenas cerca de 3 % da massa celular tumoral, esta população celular mostrou-se responsável pelo processo tumorigénico e pela diferenciação tumoral, sendo-lhe deste modo imputadas a heterogeneidade tumoral, a resistência à quimio- e radioterapias e as recidivas tumorais. Alguns autores chegam mesmo a propor que são estas as células responsáveis pela doença metastática.

O presente trabalho mostra que, como previamente sugerido na literatura, as CETs podem ser formadas por dediferenciação de células tumorais diferenciadas, sob condições de stresse. No sistema celular que implementamos, a privação de oxigénio e nutrientes quando as células tumorais foram injetadas no compartimento subcutâneo de ratinhos imunocomprometidos, foi suficiente para activar fibroblastos não malignos do estroma levando-os a estabelecer com as células tumorais uma comunicação parácrina mediada pela Interleucina-6 (IL-6), a Activina-A e o Fator Estimulador de Colónias de Granulócitos (G-CSF), a qual regulou a formação subsequente do tumor e a sua diferenciação celular. Mais ainda, o mesmo sistema permitiu perceber que as citocinas em causa foram libertadas no interior de exosomas e deste modo, que o bloqueio da libertação de exosomas e/ou a remoção das citocinas do meio, impedem a dediferenciação celular.

Trata-se da primeira vez que exosomas são implicados na dediferenciação de CETs, o que representa uma nova e promissora área de investigação, bem como um potencial novo foco para o desenvolvimento de terapias anticancerígenas dirigidas.

Agradecimentos

Em primeiro lugar, e como não poderia deixar de ser, quero expressar os meus mais sinceros agradecimentos à **Professora Carmen Alpoim**. Esta nossa caminhada já vai longa! E é incrível como continuo a adorar fazê-la, e a aprender consigo a cada passo do caminho. Obrigado por todos os ensinamentos, pela paciência, pelos desafios propostos. Obrigado pela ajuda, pelos conselhos e pela confiança. Mas acima de tudo, obrigado pela amizade! Não é o fim do livro; apenas o início de um novo capítulo.

À **Fundação Portuguesa para a Ciência e Tecnologia (FCT)** e ao **Centro de Investigação em Meio Ambiente, Genética e Oncobiologia (CIMAGO)** um agradecimento especial pelo investimento efetuado.

Há um percurso mais ou menos linear para quem permanece na Academia! É-se aluno, evolui-se no estatuto, eventualmente tornamo-nos Post-doc e temos alunos. O melhor de tudo, descobri eu, é quando esses alunos se transformam em colegas, e os colegas em amigos. **Eurico Serrano** és um exemplo disso! Acompanhar e participar ativamente na tua formação foi um privilégio. Obrigado pelo imenso trabalho e empenho que depositaste neste trabalho.

A todos os autores deste manuscrito e a todas as outras pessoas que não tão diretamente nele estiveram envolvias, terão sempre a minha gratidão.

Aos meus **Amigos**. Os de sempre e que serão certamente para sempre; àqueles que são família, um enorme OBRIGADO! Sem vocês não seria o que sou hoje.

Mãe e **Pai**, mais um fruto do vosso trabalho! Talvez o mais inesperado. Obrigado por me terem apoiado em mais uma aventura e por serem sempre o meu porto de abrigo. Amo-vos com todo o meu coração!

Contents

List of Figures

List of Tables

List of Abbreviations

^{18}FDG - [^{18}F]-fluoro-2-deoxyglucose.

α -SMA - α-smooth muscle actin.

ANOVA - Analysis of variance.

bFGF - Basic fibroblast growth factor.

CDn - Cluster of differentiation n.

CETs - Células estaminais tumorais.

Cis - Cisplatin.

CHUC - Centro Hospitalar Universitário de Coimbra.

CNC - Centro de Neurosciências e Biologia Celular.

Cr(VI) - Hexavalent chromium.

CSCs - Cancer stem cells.

DAPI - 4',6-Diamidino-2-phenylindole.

DMSO - Dimethyl sulfoxide.

DNA - Deoxyribonucleic acid.

DGAV - Direção-Geral de Alimentação e Veterinária.

DT - Duplication time.

EGF - Epidermal growth factor.

ELISA - Enzyme-linked immunosorbent assay.

EMT - Epithelial to mesenchymal transition.

EU - European Union.

FBS - Fetal bovine serum.

G-CSF - Granulocyte colony-stimulating factor.

Gem - Gemcitabine.

HBF - Human bronchial fibroblasts.

HLA - Human leukocyte antigen.

IL-6 - Interleukin 6.

ITS - Insulin, transferrin and selenium pyruvate solution.

mAb(s) - Monoclonal antibody(ies).

MTT - 3-[4, 5-dimethylthiazol-2-yl]-2, 5-diphenyltetrazolium bromide.

MTX - Methotrexate.

NGFR - Nerve growth factor receptor.

OCT-3/4 - Octamer-binding protein ¾.

ORBEA - Órgão Responsável pelo bem-estar animal.

PBS - Phosphate-buffered saline.

PE - Plating efficiency.

Poly-HEMA - Poli-(2-hydroxyethyl methacrylate).

Rpm - rotations per minute.

RT - Room temperature.

SCs - Stem cells.

SEM - Standard error of the mean.

SFA - Sphere forming assay.

STAT3 - Signal transducer and activator of transcription 3.

Introduction

Tumors are dynamic and heterogeneous entities that act like organs in a perfect trading with the entire body. They are comprised of distinct cell populations that can either be the direct product of cells with different cellular or embryonic origins, or a byproduct of the asymmetric division of stem-like cells. In agreement, cancer-committed stem-like cells, often termed CSCs, have been identified virtually in all solid and hematological tumors (1).

CSCs share several similarities with normal adult stem cells (SCs), including self-renewal capacity, expression of pluripotency surface markers and multilineage differentiation properties (2), but unlike them, CSCs have sustained cellular proliferation (3). Their tremendously variable frequency among the different tumor types, and within tumors of the same origin, makes them difficult to ascertain (4). They were initially thought to develop from the pre-existing normal tissue SCs following exposure to molecules secreted by the tumor (5), but there is now consensus that CSCs may arise either directly following transformation of normal tissue SCs or by dedifferentiation of non-SCs (6), for instance following epithelial to mesenchymal transition (EMT) (7, 8), or radiochemotherapy, as recently reviewed by Chen and collaborators (9).

Exploiting the recently evoked involvement of cytokines and soluble molecules in keeping and inducing CSCs' phenotype may constitute a new molecule-focused therapeutic opportunity. In this line, using an elegant cell culture model previously developed in the laboratory we were able to show that IL-6, Granulocyte colony-stimulating factor (G-CSF) and Activin-A released by stroma fibroblasts drive lung carcinoma cells' dedifferentiation and CSCs formation. Moreover, it was possible to ascertain a specific role to each cytokine as well as to establish the dynamics of the cytokines' release. The attained results present a new avenue for therapeutic intervention aiming CSCs ablation and metastasis abrogation.

Material & Methods

1.1 Cells and Cell Culture

RenG2 cells are a malignant cellular system previously produced in our laboratory (10), maintained in LHC-9 medium (Gibco) at the initial cellular density of $0.1x10^6$ cells/cm^2, unless otherwise stated. The derivative (DRenG2 and DDRenG2) and the stem (SC-DRenG2, SC-DDRenG2 and iRenG2) systems were attained as abovementioned and kept in DMEM:F12 (1:1) medium (Gibco) supplemented with 5 % penicillin (5000 U/mL)-streptomycin (5000 µg/mL) (Gibco), 5 % Insulin-Transferrin-Selenium pyruvate (ITS) solution (Gibco), 0.1 % amphotericin (Gibco), 0.6 g of sodium bicarbonate (Sigma-Aldrich) and 0.08 g of putrescine (Sigma-Aldrich).

A mouse fibroblats primary cell line, FR, was attained using a protocol adapted in our laboratory by surgically removing cells from the thoracolumbar aponeurosis of BALB/c-nu/nu mice (Charles-River). Isolated tissue was fragmented, and the attained small pieces distributed throughout the basis of a cell culture flask (SPL-Biosciences). A drop of fetal bovine serum (FBS) was added to each of the fragments to help them adhering and to provide them with nutrients. Finally, the flask was turned upside-down and DMEM medium (Gibco) supplemented with 10 % FBS (Gibco) was added to the top surface of the flask. Fragments were allowed to attach upside-down for 24 h and then the flask was gently

turned to the up right. After monolayer formation the cells were disaggregated, sub-culture and amplified, yielding the FR cellular system. The human bronchial fibriblasts (HBF) cell line was developed using the same protocol but from non-malignant human lung tissue attained from a patient at the CHUC, through appropriate informed consents and after the approval by the hospitals' ethics committee.

For co-culture experiments a fibroblasts feeder layer of either FR or HBFs cells were cultured in a 6 well plate (SPL-Biosciences) equipped with 4.5 cm^2 Transwell insert (Corning) containing RenG2 cells.

1.2 Tumorigenic Assays

In vivo tumorigenic assays were performed in NOD scid gamma mice (Charles River) by subcutaneously injecting $5x10^6$ cells into the flank region of the animals. Mice were housed under standard conditions at the CNC animal facility and screened twice a week for tumor formation. All animal procedures were conducted according to the EU Directive 2010/63/EU for animal experiments and reviewed and approved by DGAV, ORBEA and the animal facility ethics committee.

1.3 Duplication Times Calculation

Duplication times (DTs) were attained using previously established 3-[4, 5-dimethylthiazol-2-yl]-2, 5-diphenyltetrazolium bromide (MTT) assay protocols (11) and calculations were performed in the Doubling Time software at Doubling Time webpage (12).

1.4 [^{18}F]-fluoro-2-deoxyglucose uptake

1.5 mL of single-cell suspensions containing 2x10^6 cells/mL were attained from either adherent-growing cell lines or tridimensional spheres. The suspensions were placed in 10 mL centrifuge tubes (SPL-Biosciences) and left for recovery for 1 h at 37 ºC. Subsequently, a calculated volume of 37 ºC-heated [^{18}F]-fluoro-2-deoxyglucose (^{18}FDG) was added to reach a final concentration of 0.75 MBq/m, tubes were homogenized and conserved at 37 ºC. After 1 h incubation, samples of 200 µL were collected to 1.5 mL microcentrifuge tubes (SPL-Biosciences) containing 500 µL of ice-cold phosphate-buffered saline (PBS) (Sigma-Aldrich). Tubes were then centrifuged 1 minute at 10 000 rpm and the supernatants were collected into glass tubes. 500 µL of ice-cold PBS (Sigma-Aldrich) were added to the pellets to wash any remaining radioactive medium and tubes were again centrifuged. Supernatants were collected to the same glass tube as previous and cell pellets were preserved. Finally, both the supernatants and the pellets were assayed for radioactivity using a Radioisotope Calibrator Well Counter (CRC-15W Capintec) narrowed to the ^{18}F sensitivity energy window (400-600 keV). All cell populations were studied in triplicate in at least three sets of independent experiments. The attained results represent the percentage of cells' radioactivity relatively to the total radioactivity added, normalized per million of cells.

1.5 Clonogenic Assays

13 cells/cm^2 cells were plated onto 100 mm Petri dishes (SPL-Biosciences), allowed to grow for 15 days and then fixed and stained with crystal violet (Sigma-Aldrich) according to the protocol established by the group of van Bree (13). Surviving colonies containing more than 10 cells were scored to assess cloning efficiency and the complete protocol was repeated at least three times. Plating efficiency (PE) was calculated dividing the number of colonies formed by the number of cells seeded and the results were presented as a mean ± SEM of three independent assays.

1.6 Scratch Migration Assay

4x10^3 cells/cm^2 were added to 60 mm cell culture dishes (SPL-Biosciences) and allowed to reach confluence. After a linear scratch was performed using a p200 pipet tip, the cultures were washed and an experimental site was defined in each dish. Cells were allowed to grow, and photographs were taken at 0 h, 12 h, 19 h, 24 h, 27 h, 37 h, 49 h, 60 h, 73 h, 82 h, 93 h, 176 h and 200 h using a Moticam 2300 3.0 M Pixel USB 2.0 camera (Motic) coupled to a AE31 microscope (Motic).

1.7 Drug-resistance Assays

Single-cell suspensions of all the five cell lines proliferating or attained from the dissociations of spherical clones were plated into a 24-well plates at an optimized initial cellular density of 8x10^3 cells/cm^2. 24 h after cells' seeding, 10 μL of each drug solution [cisplatin (Cis, CG6413, Generis), methotrexate (MTX, Teva Pharmaceutical Industries)

and gemcitabine (Gem, Gemzar, Lilly) were administered to attain the desired final concentration (0.0 μM, 0.1 μM, 10 μM and 50 μM). For each condition, including the controls, three independent assays were carried in triplicate. Cells' viability was assessed every 24 h, during 3 days using the MTT reduction assay.

1.8 CSCs' isolation – Sphere Formation Assay

CSCs' isolation was performed using the sphere formation assay (SFA). To that end low adherence 6-well plates (SPL-Biosciences) were prepared by coating the plates' surface with a 2 % poli-(2-hydroxyethyl methacrylate) (poli-HEMA). The isolation medium consisted of a 1:1 mixture of the CSCs maintaining medium with a 2 % methylcellulose (Sigma-Aldrich) solution. For the isolation, 2 mL of a cellular suspension containing $3x10^4$ cells/mL were added to each well and the isolation medium was supplemented with 10 ng/mL of both human epidermal growth factor (EGF) (Sigma-Aldrich) and basic fibroblasts growth factor (bFGF) (PeproTech). Cells were allowed to grow and supplements' concentration was replaced every two days. Spheres formation was accompanied and photographed along time, and 15 days after platting they were collected, washed with PBS, and plated in T_{25} cell culture flasks (SPL-Biosciences) provided with 5 mL fresh maintaining medium. Cells were allowed to attach and expand, and the protocol of isolation was repeated twice when they reached nearly 80 % confluence.

1.9 Immunocytochemistry

$4x10^3$ cells/cm^2 were seeded on the top of microscope slides (VWR) placed inside a 100 mm cell culture dish (SPL-Biosciences) and cells were allowed to grow until approximately 80 % confluence. Following medium aspiration the slides were rinsed twice with PBS (Sigma-Aldrich), collected into centrifuge tubes (SPL-Biosciences) containing 50 mL of 95 % ethanol (Sigma-Aldrich) and kept overnight at 4 ºC. To quench the endogenous peroxidase activity 15 minutes incubation was performed in a 3 % hydrogen peroxide (H_2O_2) solution. Subsequently preparation steps were performed using the Ultra Vision Kit (Thermo Scientific), according to manufacturers' instructions. After dehydration, slides were mounted using the Tissue-Tek Glas Mounting Medium (1408, Sakura).

Vimentin was stained using the Vim3B4 primary antibody (Dako Corporation), α-smooth muscle actin (α-SMA) the αSM-1 (Leica Biosystems), octamer-binding protein ¾ (OCT3/4) with the N1NK (Leica Biosystems) and β-catenin with CAT-5H10 (ThermoFisher Scientific). 4',6-Diamidino-2-phenylindole (DAPI) staining was used to mark the nuclei. Cells' were observed in a Nikon Eclipse 80i microscope and photographs were taken using a Nikon Digital DXM1200F coupled camera.

1.10 Flow Cytometry-based Cellular Characterization

Four different cytometry tubes containing 300 µL of $1x10^5$ cells single-cell suspensions were prepared per cellular system, two tubes for the blank controls and the other to be incubated with the selected panel of fluorescence-labeled monoclonal antibodies (mABs) as schematized in Table I. The mABs used were cluster of differentiation 31

(CD31) (WM59, BD Biosciences), nerve growth factor receptor (NGFR) (C40-1457, BD Biosciences), CD14 (M5E2, BD Biosciences), CD13 (Immu103.44, Beckman Coulter), CD133 (293C3, Miltenyi Biotec), CD11b (ICRF44, BD Biosciences), CD45 (HI30, Invitrogen), CD106 (51-10C9, BD Biosciences), CD105 (1G2, Beckman Coulter) and human leukocyte antigen (HLA) A, B, C (G46-2.6, BD Biosciences). The volumes of each mAB were selected according to manufacturer's recommendations and are listed in Table I.

Table I - Markers and fluorophores used in the flow cytometry-based cellular characterization studies.

	Tube 1		Tube 2	
FITC	CD31	10 µL	CD106	10 µL
PE	NGFR	10 µL	CD30	10 µL
PerCP5.5	CD14	2.5 µL	-	-
PeCy7	CD13	2.5 µL	CD13	2.5 µL
APC	CD133	10 µL	HLA-A,B,C	10 µL
PB	CD11b	2.5 µL	CD11	2.5 µL
PO	CD45	2.5 µL	CD45	2.5 µL

FITC - Fluorescein isothiocyanate; PE - Phycoerythrin; PerCP - Peridinin-cholophyll-protein complex; PeCy7 - Phycoerythrin Cy7-conjugated; APC - Allophycocyanin; PB - Pacific blue; PO - Pacific orange.

Cells were incubated 15 minutes with the mABs in the dark at room temperature (RT), rinsed with 2 mL of PBS (Sigma-Aldrich) and centrifuged for 5 minutes at 1500 rpm. Pellets were ressuspended in circa 200 µL of the supernatant and sample readings were carried out in a FACS Canto II Flow Cytometer (BD Biosciences). The attained results were analyzed using the CellQuest software (BD Biosciences).

1.11 Enzyme-linked Immunosorbent Assay

Enzyme-linked Immunosorbent Assays (ELISA) were performed following manufacturers' instructions using the Human/Mouse/Rat Activin-A Quantikine ELISA Kit (#DAC00B, R&D Systems), the Human IL-6 Quantikine ELISA Kit (#D6050, R&D Systems) and the Human G-CSF Quantikine ELISA Kit (#DCS50, R&D Systems).

1.12 Multiplex Analysis

FR cells-derived cytokines were searched for performed in the conditioned media of the co-cultured cells using the Bio-Plex ProTM Mouse Cytokine 23-plex Assay Kit (#M60-009RDPD, BioRad), according to manufacturers' instructions. Samples were studied in triplicate in a Bio-Plex 200 System (BioRad), and the attained results were analyzed using the Bio-Plex ManagerTM Software, Standard Edition (BioRad).

1.13 Exosomes' Isolation, Permeabilization and Uptake Blockage

Exosomes' isolation was performed using the protocol established by Raposo and collaborators (14). Briefly, successive centrifugations at increasing speed were used to eliminate large cellular debris and the final supernatant is ultra centrifuged at 100 000 G for 70 minutes to pellet the exosomes. The pellet was then washed abundantly with PBS (Sigma-Aldrich) to eliminate contaminating proteins, and centrifuged one last time at the same high speed (15).

Permeabilization followed the protocol designed by Subra and colleagues (16), according to which 50 μg of exosomal protein were incubated with 5 μL protease inhibitor cocktail (Sigma-Aldrich) in 1 mL of PBS (Sigma-Aldrich) for 10 minutes at RT, and then sonicated 2x 10 seconds (VWR Ultrasonic Cleaner).

Exosomes' uptake blockage was attained by adding a 50 mg/mL xyloside alcoholic solution to the cell culture medium. The solution was attained by dissolving 0.1 g of xyloside (Sigma-Aldrich) in 2 mL of methanol (Sigma-Aldrich).

1.14 Statistical Analysis

Unless stated otherwise, results derive from at least three independent experiments carried out in triplicate, and their statistical analysis was carried out using the Graph Pad Prism software version 7 (GraphPad Inc.). Error bars indicate ± SEM between biological replicates. Statistical significance of multiple-group comparisons was attained using one-way ANOVA with Bonferroni post hoc analysis. A p value < 0.05 was defined as the threshold of significance and the P value was categorized according to their interval of confidence.

Results & Discussion

in vivo cellular derivation increased cells' malignant potential

The malignant RenG2 cell line was established by culturing the non-malignant immortalized human bronchial epithelial cells BEAS-2B at extremely low density in the presence of 1.0 μM hexavalent chromium [Cr(VI)]. As a control, Cont1 cell line was attained from low-density Cr(VI)-free cultures (10). Although malignant, RenG2 cells needed about two months to induce tumor formation in immunocompromised mice, so their malignant potential was increased by *in vivo* derivation using serial rounds of injection in immunocompromised mice. As a consequence, DRenG2 cells were attained from primary cultures of the RenG2-induced tumor and the DDRenG2 cells from primary cultures of the DRenG2-induced tumor (Figure 1A). Relative tumorigenic ability comparison confirmed the progressively increased malignancy of the derived systems (Figure 1B).

Supporting the *in vivo* studies, DTs calculation showed that the malignant cell lines replicate faster than non-malignant ones, particularly DRenG2 cells which showed a DT of roughly 18.5 h (Figure 1C). No statistically significant differences were observed between DDRenG2 and either RenG2 or DRenG2 cells, and the results attained for BEAS-2B cells corroborated prior studies of Costa and colleagues by documenting a DT of approximately

23 h (17). Cont1 cells showed no statistically significant differences in their DTs when compared to BEAS-2B, thus presenting them as a good experimental control.

Consistent with previous observations showing that malignization is accompanied by an increase in glucose uptake and a stimulation of aerobic glycolysis (18-20), the comparative study of ^{18}FDG-uptake showed that the malignant cell lines had a considerably higher glucose demand than the non-malignant ones (Figure 1D). However, as malignancy increased the glucose uptake decreased. Moreover, malignant systems displayed a progressively higher clonogenic capacity (Figure 1E), higher migration ability (Figure S1) and an increased cell survival following treatment with conventional lung carcinoma-directed drugs, namely cisplatin, methotrexate and gemcitabine (Figure 1F). In fact, both derivative systems distinctively succeed in surviving the entire repertoire of employed drugs, particularly DDRenG2. Altogether the attained results confirmed the malignant nature of both RenG2 and their progeny by identifying features consensually ascertained to malignant cells.

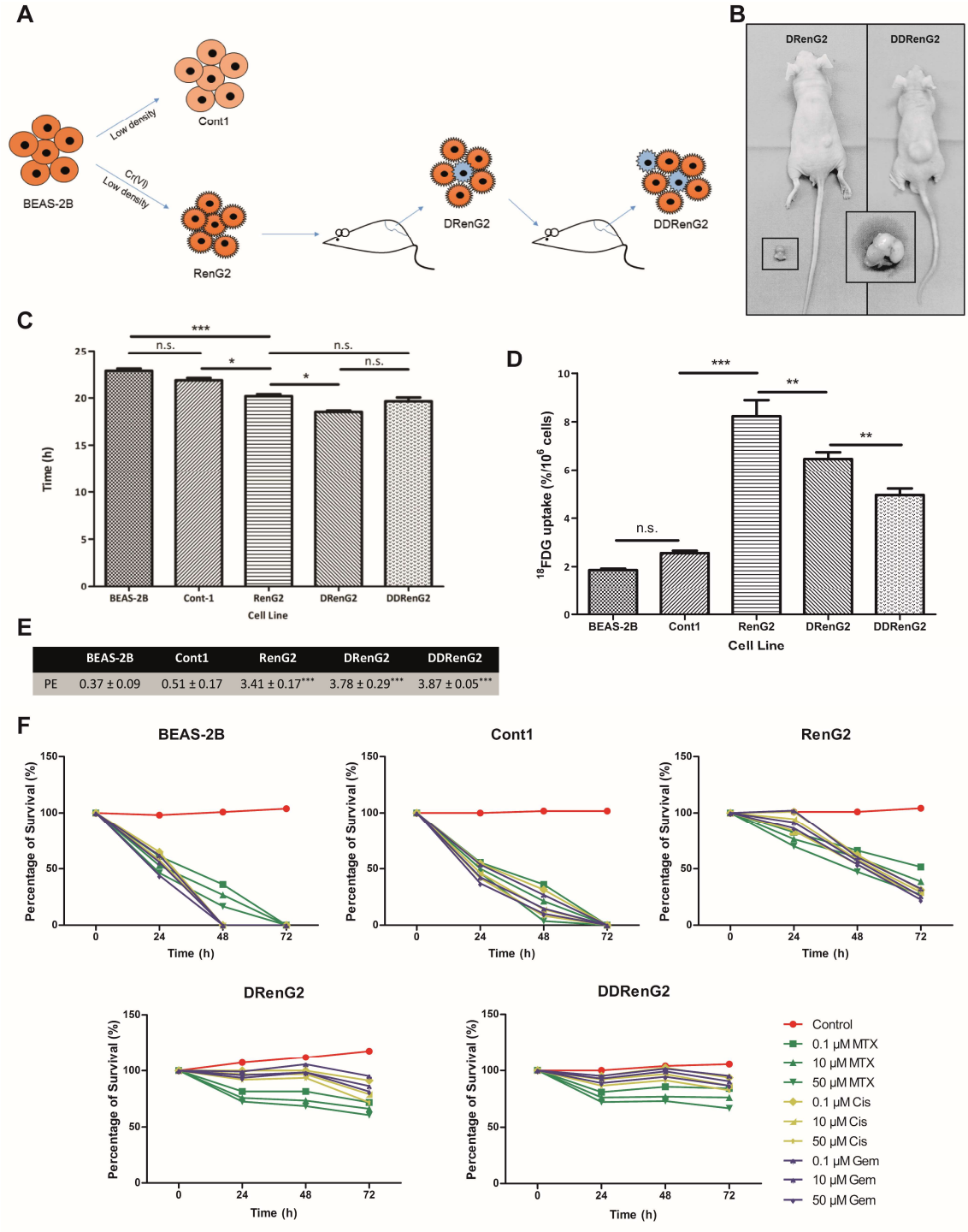

Figure 1 – RenG2 cells' *in vivo* derivation increased their malignant potential. **(A)** Derivation experimental protocol. **(B)** Comparative tumorigenic potential of the derivative cellular systems. Tumors induced by the same number of cells in the same experimental period, clearly depicting DDRenG2' higher malignant potential. **(C)** Cellular duplication times. Malignant cells replicated significantly faster than their non-malignant progenitors. RenG2 DT was significantly different from that of DRenG2 cells, while no

significance was observed when comparing DDRenG2 to its malignant counterparts. **(D)** ^{18}FDG uptake. Malignant cells showed a considerably higher glucose uptake. Unexpectedly, however, as malignancy increased the glucose uptake decreased. **(E)** Plating efficiency. Malignant cells exhibited a considerably higher plating efficiency. **(F)** Drug-resistance assays. The higher the degree of malignancy, the higher the resistance to the different drugs, at all tested concentrations. Derivative cell lines, in particular, were shown to be more sensitive to MTX than their non-malignant progenitor cells. MTX, methotrexate; Cis, cisplatin; Gem, Gemcitabine. Data represents mean ±SEM. Differences between the means were evaluated by one-way ANOVA followed by a Bonferroni post test. n.s., no significant; *, $P \leq 0.05$; **, $P \leq 0.01$; ***, $P \leq 0.001$. For PE a Bonferroni post test was used.

Malignant potentiation was underlined by CSCs formation

Medema's laboratory proposed that only CSCs are endowed with tumorigenic capacity and the ability to resist chemotherapy (21). By interpreting the previous results in light of Medema's theory, it became plausible to hypothesize that CSCs mediated BEAS-2B cells' malignization and were liable for the malignant features of RenG2, DRenG2 and DDRenG2 cell lines. To test this hypothesis the SFA along with immunocytochemistry was performed. SFA constitutes a reliable method to specifically isolate CSCs from inside a heterogeneous mixture of cells while preserving the key characteristics of the original patient tumors (4). Immunocytochemistry, instead, allows monitoring EMT, a proposed source of CSCs (22), as the lost of epithelial features towards a mesenchymal phenotype triggers the expression of α-SMA and increases that of Vimentin (23).

Basal levels of Vimentin staining were found in BEAS-2B and Cont1, illustrating the ubiquitousness of this protein (Figure 2A). The malignant systems, however, showed an increased expression of Vimentin, thus revealing their mesenchymal phenotype and explaining their increased motility, which according to Mendez and collaborators, is the result

of the assembly of Vimentin intermediate filaments (24). Not surprisingly, α-SMA was only expressed in the malignant cell lines, not only corroborating the epithelial nature of both BEAS-2B and Cont1, but also suggesting the stem potential of the malignant systems (Figure 2A). SFA, however, only yielded spheres when either DRenG2 or DDRenG2 cell lines were cultured at restraining conditions (Figure 2B and 2C), and the spheres attained with DDRenG2 cells were not only bigger but also more numerous than those formed by DRenG2 (Figure 2D). This observation imprinted a higher stem potential to the DDRenG2 cellular system and further suggested that the CSCs isolated from DRenG2 cultures were obtained through dedifferentiation of RenG2 cells and not by transformation of endogenous stem-like cells. The resulting DRenG2 and DDRenG2 spheres were purified after 3 generations of isolation and CSC lines were established out of each of the derivative systems and respectively named SC-DRenG2 and SC-DDRenG2.

New relative characterization of the attained CSCs lines showed that the glucose requirements of the CSC systems were comparable to those of non-malignant BEAS-2B and Cont1 cells, and thus significantly lower than any of the malignant progenitor cell lines (RenG2 cells included) (Figure 2E). However, MTT-based cell DTs' calculations revealed that the modest glucose necessities of CSCs portrayed their quiescent status, as these cell populations have a considerably longer cell cycle than their progenitors (Figure 2F). Furthermore, methotrexate-resistance studies showed that, contrarily to what was observed to the progenitor malignant systems, drug treatment failed to abrogate CSCs' cycle progression, as the cells kept dividing in the presence of the drug (Figure 2G). This higher resistance of CSCs to therapy is in line with previous observations (25-28) and is thought to be the main responsible for quiescence (29, 30). In fact, as many chemotherapy agents

require cell cycle progression to act, CSCs' avoid death by entering quiescence and inducing a very efficient activation of the deoxyribonucleic acid (DNA) repair genes, as well as an overexpression of drug efflux pumps (6, 28, 31).

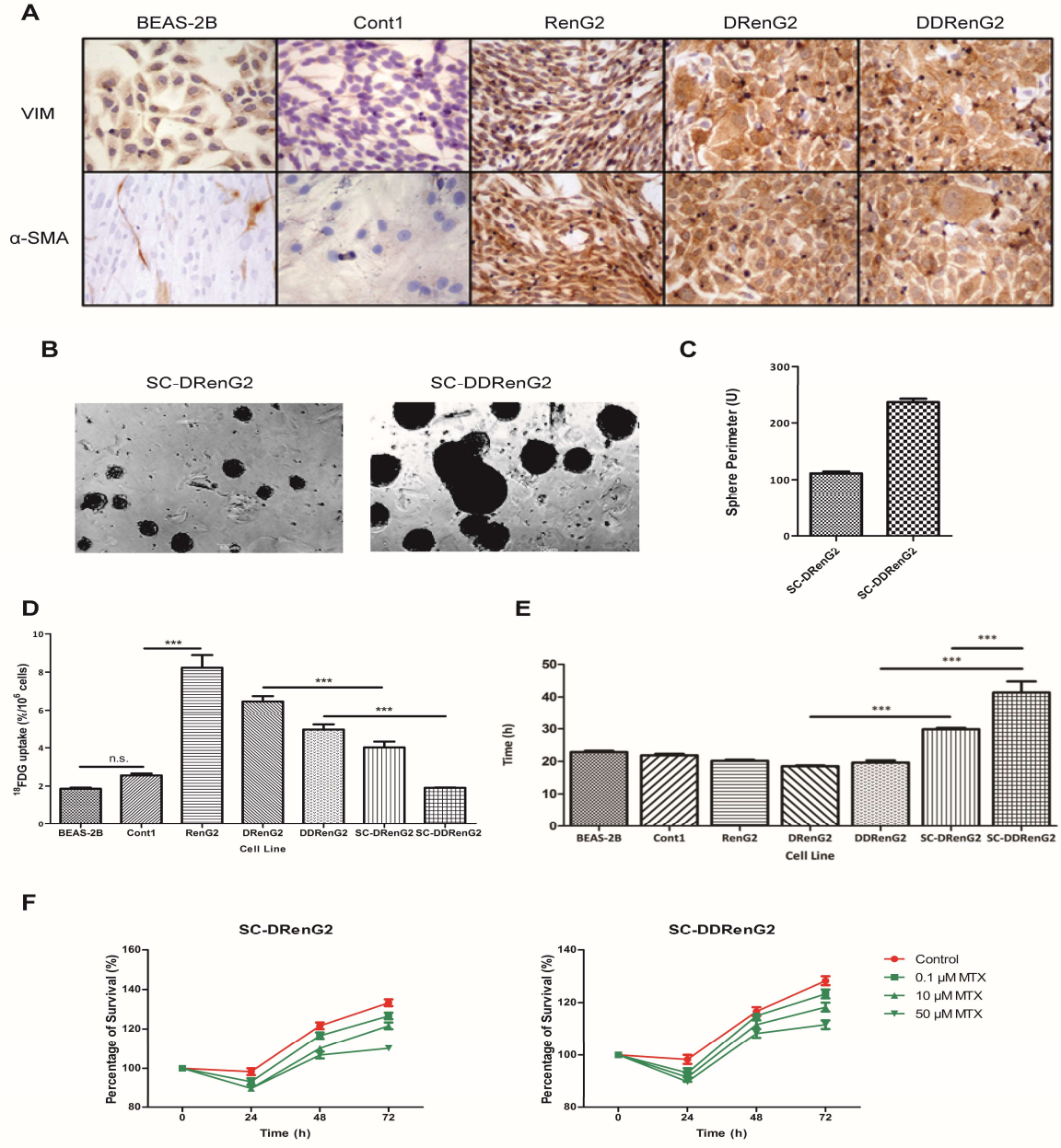

Figure 2 – RenG2 cells' derivation featured CSCs formation by dedifferentiation. (A) Immunocytochemistry study of Vimentin and α-SMA. Both BEAS-2B and Cont1 non-malignant systems displayed a basal staining for Vimentin. Conversely, α-SMA staining was negative in these cell lines. All the malignant systems, however, presented a strong staining for both Vimentin and α-SMA. A magnification of

400x was used in all panels. VIM, Vimentin. **(B)** SFA from the derivative systems. DDRenG2 cell line formed more and larger spheres than its progenitor, the DRenG2 cell line. A magnification of 100x was used in both photographs. **(C)** Perimeter analysis of the spheres formed by both derivative systems. 50 spheres were measured per analyzed cell line. **(D)** Comparative analysis of ^{18}FDG uptake. Both SC-DRenG2 and SC-DDRenG2 cell lines uptake significantly less ^{18}FDG in comparison to the other malignant cell lines. **(E)** Comparative study of cellular duplication times. Both SC-DRenG2 and SC-DDRenG2 had considerably higher DTs than their derivative progenitors. Moreover, SC-DDRenG2 needed even more time to replicate than SC-DRenG2. **(F)** CSCs' survival following MTX treatment. MTX not only failed at eradicating CSCs, but also was unable to block their division, as both SC-DRenG2 and SC-DDRenG2 grew in the presence of the drug. Data represent means ±SEM. Differences between the cell lines' means were evaluated by one-way ANOVA followed by a Bonferroni post test. n.s., no significant; *, $P \leq 0.05$; **, $P \leq 0.01$; ***, $P \leq 0.001$.

Dedifferentiation as a source of CSCs

The confirmation of SC-DRenG2 and SC-DDRenG2 stem potential and the observation that there was a progressive increment in CSCs sub-populations along the derivative systems concomitantly suggested that the mouse subcutaneous compartment drove and supported RenG2 cells' dedifferentiation. To further prove this hypothesis mouse cells were surgically isolated from the thoracoabdominal aponeurosis of the animals and Transwell (Corning) co-cultured with RenG2 cells for 8 weeks (the same period RenG2 cells needed to induce tumor formation in immunocompromised mice). After co-culture, CSCs were searched for and positively isolated from the RenG2 population using the SFA, and named iRenG2. The formation of spheres was observed soon after cells' platting, similarly to what was previously seen for both SC-DRenG2 and SC-DDRenG2.

To compare the isolated iRenG2 cells with their progenitors RenG2 cells and both DRenG2 and SC-DRenG2, panels of malignancy-associated genes (Figure 3A) and molecular markers (Figure 3B) were selected. The attained results showed that iRenG2 cells'

molecular signature, unlike their progenitor RenG2, was more similar to that of both DRenG2 and SC-DRenG2, thus confirming stromal cells-mediated dedifferentiation of the RenG2 cells and establishing the process as paracrinely mediated in nature. Final confirmation was attained from cytokine multiplex array (BioRad) and ELISA performed in the conditioned media of the co-cultures, which identified consistently increased levels of IL-6, G-CSF and Activin-A (Figure 3C). A proof of concept experiment was also performed to confirm the action of these cytokines over RenG2 cells by mono-culturing these cells in their presence, and the acquisition of stem properties was positively documented (Figure S2). Moreover, the attained results were reproduced using HBFs attained out of a fresh human lung sample, and the same transformation was observed.

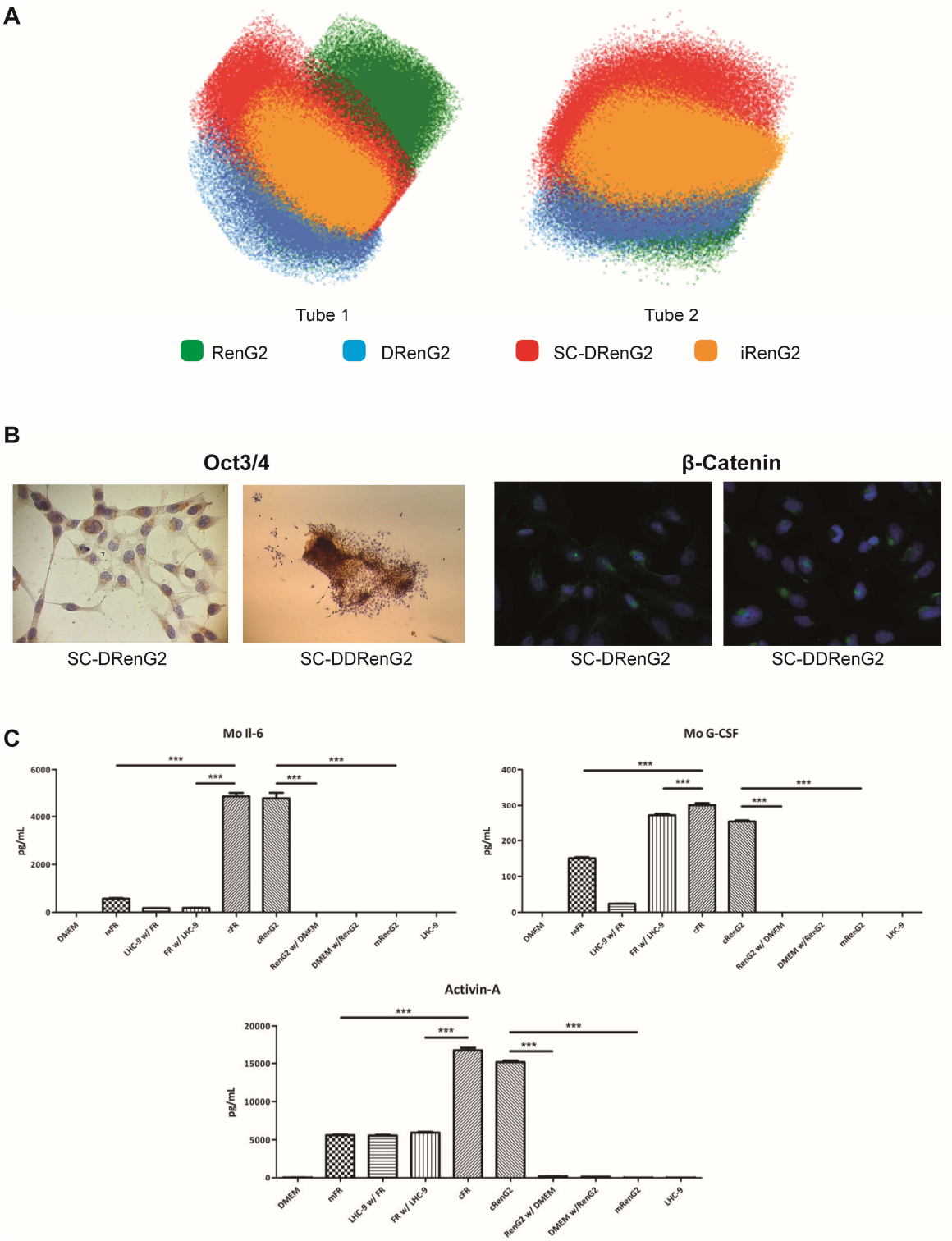

Figure 3 – Isolated CSCs' depicted classical stem properties and were attained by a cytokine-mediated paracrine loop established between the tumor cells and the micro-environment. **(A)** Flow cytometry scattering plots comparing the iRenG2 cell line to RenG2, DRenG2

and SC-DRenG2. In both tubes the yellow-represented iRenG2 cells were more close to both DRenG2 and SC-DRenG2 than to RenG2, illustrating their closer identity. Colored dots represent individual cells. RenG2 green, DRenG2 light blue, SC-DRenG2 red and iRenG2 yellow. **(B)** Immunocytochemistry study of Oct 3/4 and β-Catenin. Both CSCs systems depicted a marked staining of both proteins, with β-Catenin preferentially localized to the nuclei. A magnification of 400x was used in all panels. **(C)** IL-6, G-CSF and Activin-A levels in the conditioned media of the RenG2-FR co-culture. The cytokines' levels were significantly increased in the co-cultures relative to the controls. The use of an anti-mouse antibody allowed the detection of FR-produced cytokines in the upper compartment. Mo, mouse; mFR, monocultured FR cells; cFR, FR cells co-cultured with RenG2 cells; cRenG2, RenG2 cells co-cultured with FR cells; mRenG2, monocultured RenG2 cells; w/, co-cultured with; n.s., no significant. Data represent means ±SEM. Differences between the means were evaluated by one-way ANOVA followed by a Bonferroni post test.

Dedifferentiation-implicated cytokines are transported inside exosomes

Paracrine communication is by definition the activation of cellular signaling pathways mediated by soluble factors, which may either be freely released to the media or transported as cargos of extracellular vesicles. Among these vesicles, exosomes in particular are microvesicles of unique characteristics and composition that encapsulate material from cells' cytoplasm, thus protecting it against harsh extracellular environments (32, 33).

Hypothesizing that exosomes were involved in RenG2 cells' dedifferentiation, these microvesicles were isolated from the conditioned media of the long-term co-cultures of HBFs and RenG2 cells, and their content screened. The attained results showed a significant amount of all three cytokines' inside the exosomes isolated from the upper compartment (containing the RenG2 cells), both demonstrating that cytokine-containing exosomes were being secreted by the fibroblasts, and that these microvesicles were able to trespass the membrane of the inserts. The levels of IL-6, nonetheless, were significantly higher then those of the other cytokines, and all of them remained relatively stable along the 8 weeks

of culture (Figure 4A). The presence of the cytokines as free molecules in the conditioned media was also assessed to evaluate the impact of an eventually non-exosome mediated release. Results demonstrated the presence of basal concentrations of both IL-6 and Activin-A in both compartments, which yet remained stable along time (Figure 4B). As to G-CSF, its levels were too low above the lower calibration curve's value thus suggesting that the main release pathway of this cytokine is indeed exosome-mediated.

Performing the abovementioned co-culture experiments in the presence of the exosome-uptake blocker xyloside yielded a definitive proof of the exosome-mediated cytokines' transport and of their action over RenG2 cells. Xyloside is a small hydrophobic compound that inhibits proteoglycans' biosynthesis and whose use as an exosome-uptake blocker is quite recent (34). Its presence in the current co-culture system abrogated the acquisition of CSCs traits by RenG2 cells, which resulted in a dramatically reduction of these cells' ability to form spheres (Figures 4C and 4D).

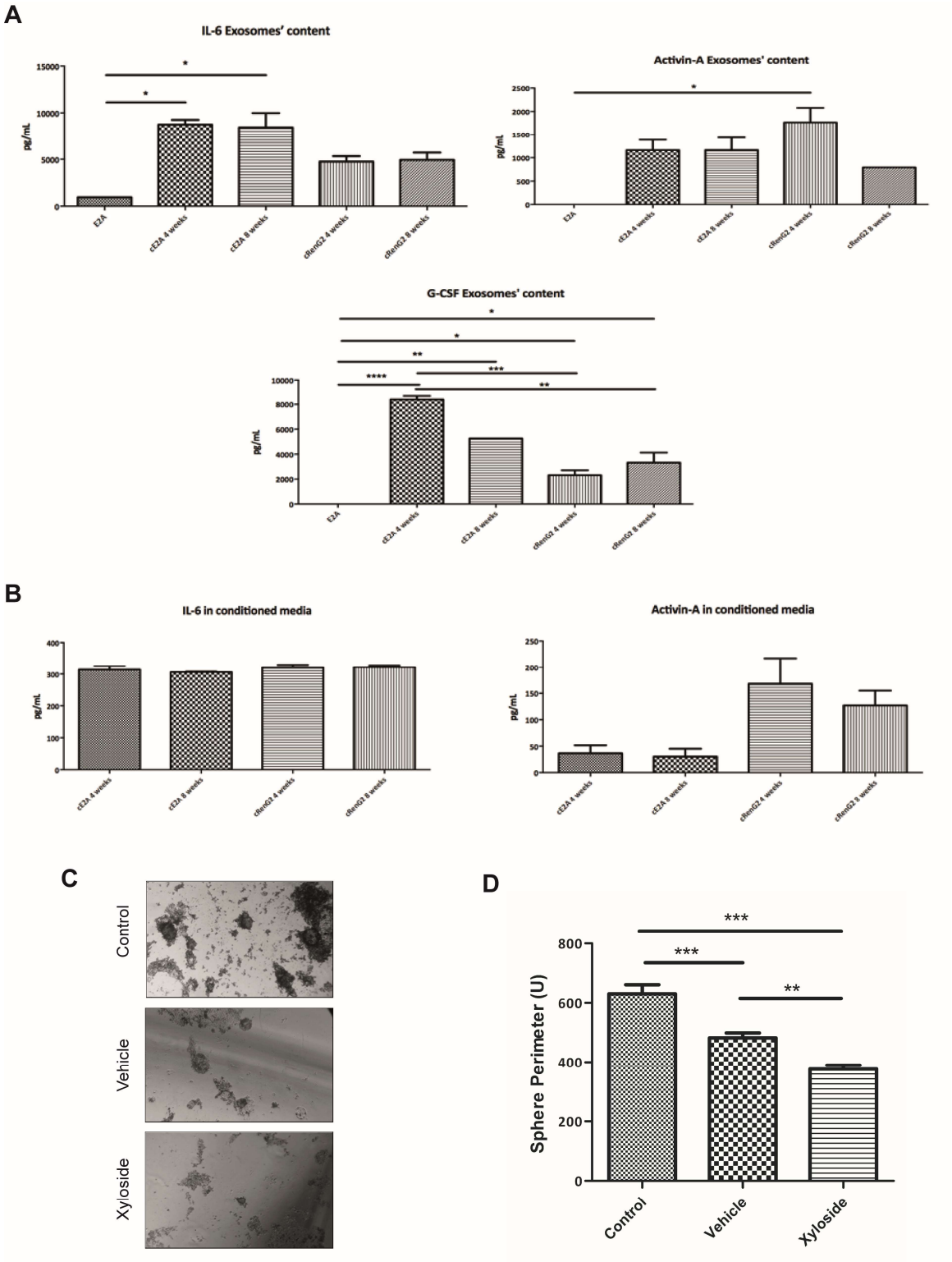

Figure 4 – Exosomes mediated the communication between tumor and stroma cells.

(A) Exosomes' content analysis. All 3 cytokines were significantly increased in the exosomes present in the upper compartment, and except for Activin-A whose levels increased along time, the remaining ones were

kept stable. **(B)** IL-6 and Activin-A levels in the co-cultures' conditioned media. The attained values were considerably lower than those find inside exosomes. Again, Activin-A levels were shown to increase in the culture media along time in culture. **(C)** SFA of RenG2 cells after co-culture with HBFs in the presence of xyloside. There was a significant reduction in the sphere-formation ability, resulting from the xyloside-mediated abrogation of exosome communication. A magnification of 100x was used in all panels. **(D)** Perimeter analysis of the attained spheres. The few attained spheres were smaller then those formed in the absence of xyloside. 10 spheres were measured per analyzed cell line. Data represent means ±SEM. Differences between the means were evaluated by one-way ANOVA followed by a Bonferroni post test.

IL-6 and Activin-A are directly involved in dedifferentiation, while G-CSF is implicated in keeping the stem phenotype.

To fully understand the dynamics of the dedifferentiation process, the impact of each individual cytokine in the overall communication process was ascertained. To this end neutralizing antibodies against IL-6, G-CSF and Activin-A were used to scavenge cytokines from the co-cultures' media, either alone or in combinations.

Corroborating the previous observations, whenever all the three cytokines were scavenged from the media, sphere formation was abrogated (Figures 5A and 5B). Also, the independent scavenge of each of the three cytokines failed to block dedifferentiation, thus showing that at least one of the three is necessary to trigger the process (Figures 5C and 5D). However, the concomitant neutralization of Activin-A and IL-6 resulted in no sphere formation, while the simultaneous neutralization of IL-6 and G-CSF yielded smaller and fewer spheres than the control co-cultures (Figures 5E and 5F). These observations showed that only IL-6 and Activin-A were endued with the ability to trigger dedifferentiation, and that IL-6 was the more potent inducer of the process. Nonetheless, they also suggested that

despite the fact that Activin-A is able to induce CSCs' formation, it seems that this cytokine may also act as a differentiation inducer of the pre-formed CSCs. In agreement, whenever Activin-A was present, the number of spheres was reduced, exception made to the situation where only this cytokine was present. Corroborating this hypothesis are several reports in the literature indicating Activin-A as a differentiation inducer (35-37).

IL-6 was the strongest inducer of dedifferentiation as more and bigger spheres formed when this cytokine was solely present (Figures 5G and 5H). This observation is in line with many recent studies performed in different tumor types, namely, gastric (38), breast (39) and bone (40), reporting that not only IL-6 is indeed able to induce dedifferentiation, but also that it does so through the activation of signal transducer and activator of transcription 3 (STAT3) and consequently, of the Notch signaling pathway (41).

The presence of G-CSF in the co-culture system, although not necessary for the dedifferentiation process, sustained of CSCs' proprieties in previously developed CSCs' pools (Figure 5C-F). This result corroborates Agarwal and colleagues' work that showed that G-CSF sustained neuroblastoma CSCs' pool through a STAT3 mechanism (42).

Altogether the attained results allow the proposal of a model for the dedifferentiation of CSCs: co-option of the stroma cells leads to an increase in IL-6 and Activin-A levels in the tumor microenvironment which in turn drive tumor cells' dedifferentiation, and consequently, CSCs' formation. Following dedifferentiation, Activin-A maintains CSCs'-pool homeostasis, inducing differentiation whenever it overcomes a certain threshold, and G-CSF provides the CSCs'-niche with the appropriate conditions to sustain the undifferentiated phenotype of its cells, by acting downstream of the previous cytokines (Figure 6).

With the accumulating knowledge on the diverse areas of cancer, the stochastic model started to be questioned. By assuming the tumor to be a mass of hyperproliferative cells equally provided with the ability to drive tumor's growth, this model justifies cellular heterogeneity and malignant progression mainly by the action of adaptive selective pressures acting over new genetic mutations or environmental alterations (Garvalov and Acker, 2011). However, evidence suggesting that tumor initiation and maintenance may only be ascribed to a limited population of cells within the tumor, along with the identification of cells with progressive degrees of differentiation shook the foundations of this theory and drove the edification of new ones.

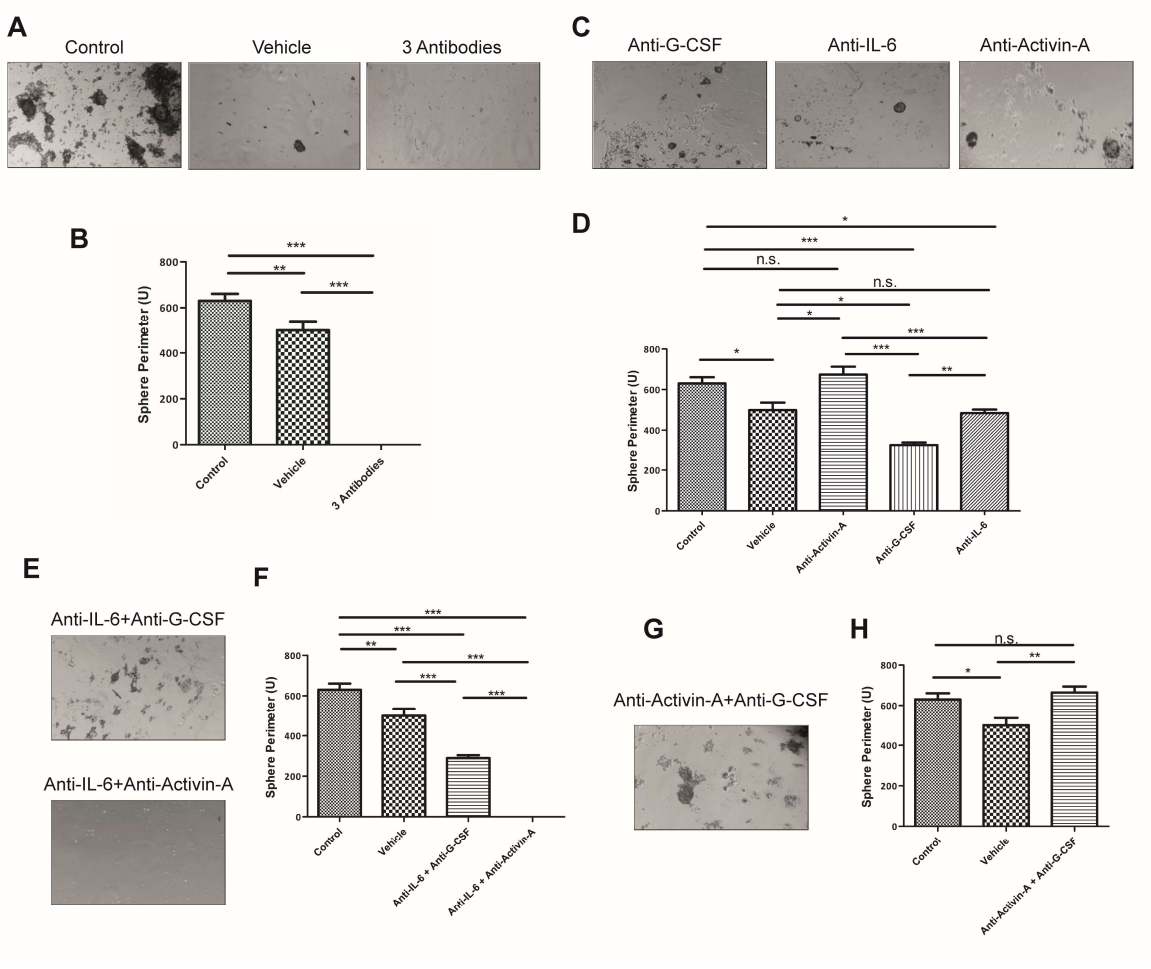

Figure 5 – IL-6 and Activin-A are the actual drivers of dedifferentiation. **(A)** SFA of RenG2 cells after co-culture with HBFs in the presence of neutralizing antibodies against IL-6, G-CSF and Activin-A. No spheres were formed. **(B)** Perimeter analysis. **(C)** SFA of RenG2 cells after co-culture with HBFs in the presence of neutralizing antibodies against IL-6, G-CSF and Activin-A, individually. Spheres were formed in all conditions. **(D)** Perimeter analysis. Bigger spheres were observed in the condition where both IL-6 and G-CSF were present in the culture media. **(E)** SFA of RenG2 cells after co-culture with HBFs in the presence of only either Activin-A or G-CSF. Activin-A was able to induce sphere formation, while G-CSF alone was unable to do it. **(F)** Perimeter analysis. Spheres formed by Activin-A were lesser and smaller than those formed when IL-6 was present. **(G)** SFA of RenG2 cells after co-culture with HBFs in the presence of only IL-6. **(H)** Perimeter analysis. IL-6 was the most potent inducer of dedifferentiation. A magnification of 100x was used in all panels. 10 spheres were measured per perimeter analysis for each cell line. Data represent means ± SEM. Differences between the means were evaluated by one-way ANOVA followed by a Bonferroni post test.

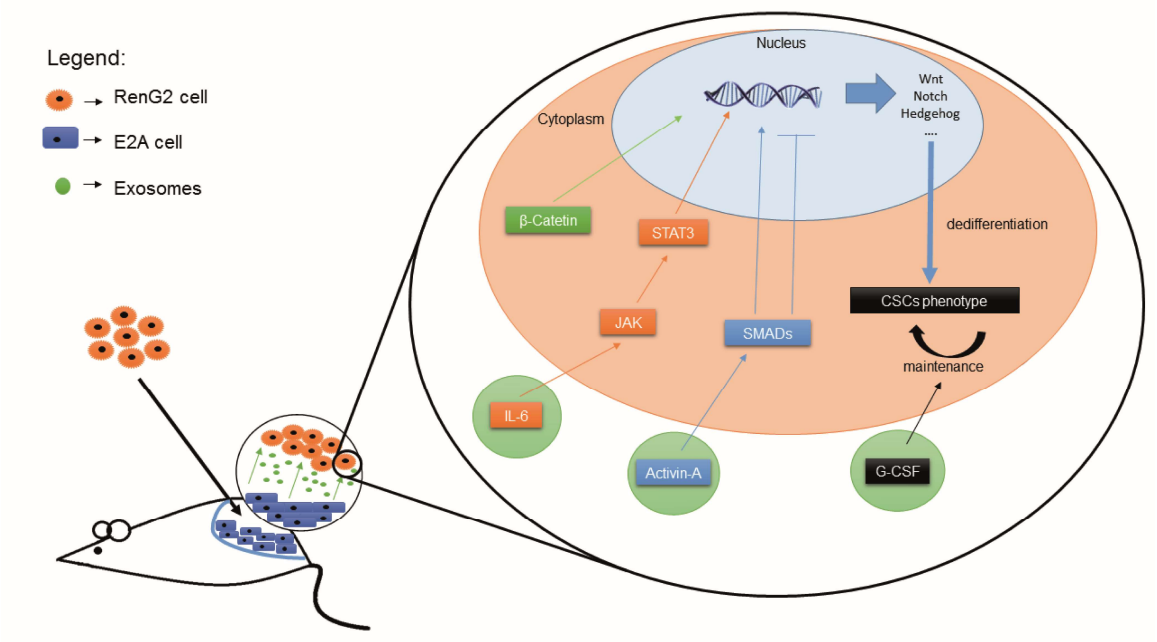

Figure 6 – Explanatory model for microenvironment-driven dedifferentiation. Fibroblasts-released exosomes containing IL-6, Activin-A and G-CSF, either combined or separated, interacted with the tumor cells inducing alteration in DNA expression, most probably through STAT3, Smad and β-Catenin activation. The consequent activation of stemness-associated pathways such as Wnt, Notch and Hedgehog drove tumor cells' dedifferentiation, which was subsequently maintained by the activity of G-CSF. Activin-A seemed to act as a sensor of the CSCs' pool homeostasis, inducing CSCs' differentiation whenever a certain threshold was reached.

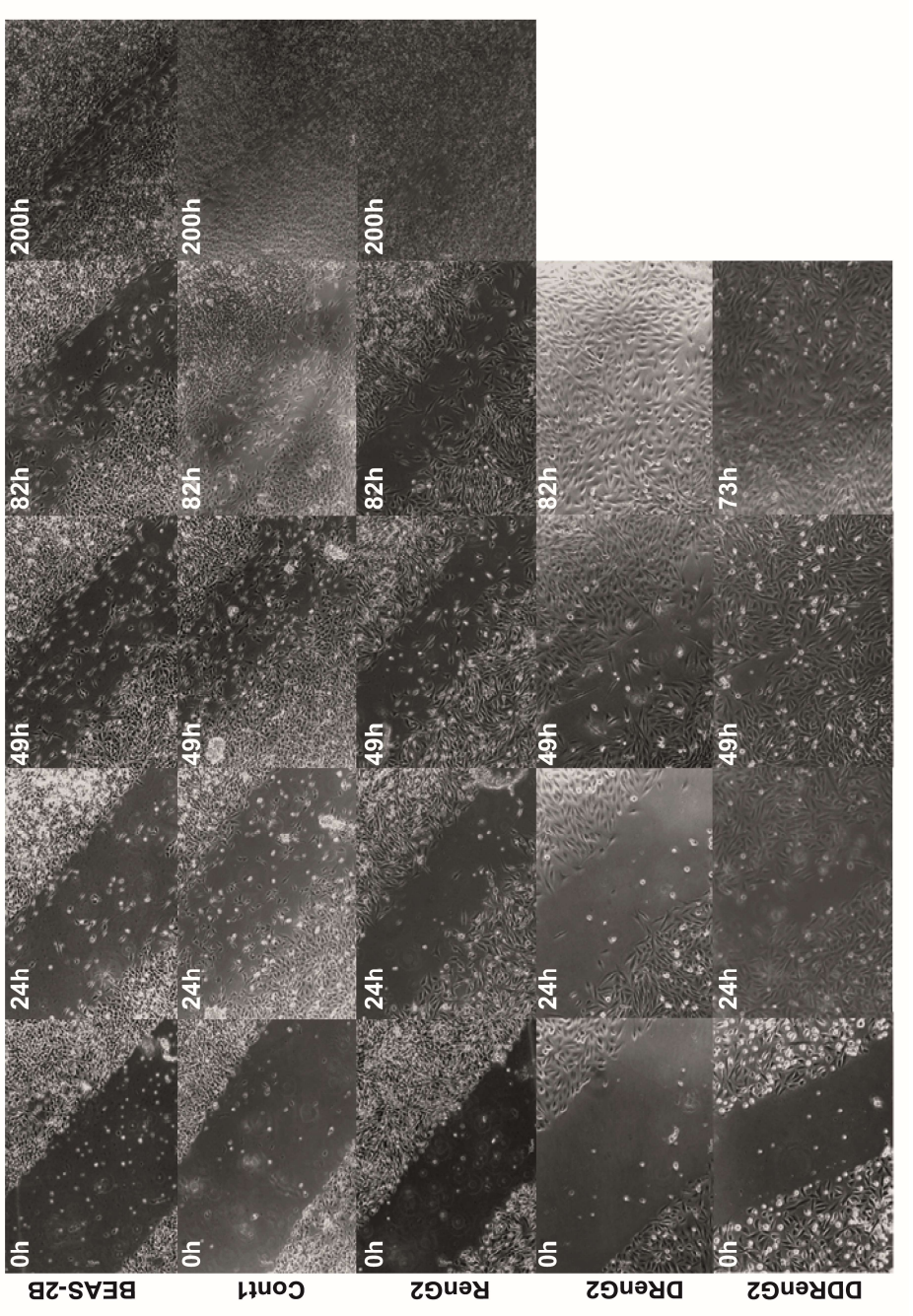

Figure S1 – Migration ability of the different cellular systems. Both BEAS-2B and Cont-1 cell lines failed to close the scratch, even after 200 h. RenG2 cells grossly closed it, but DRenG2 and DDRenG2 did it faster and better in progressively less time. A magnification of 100x was used in all panels.

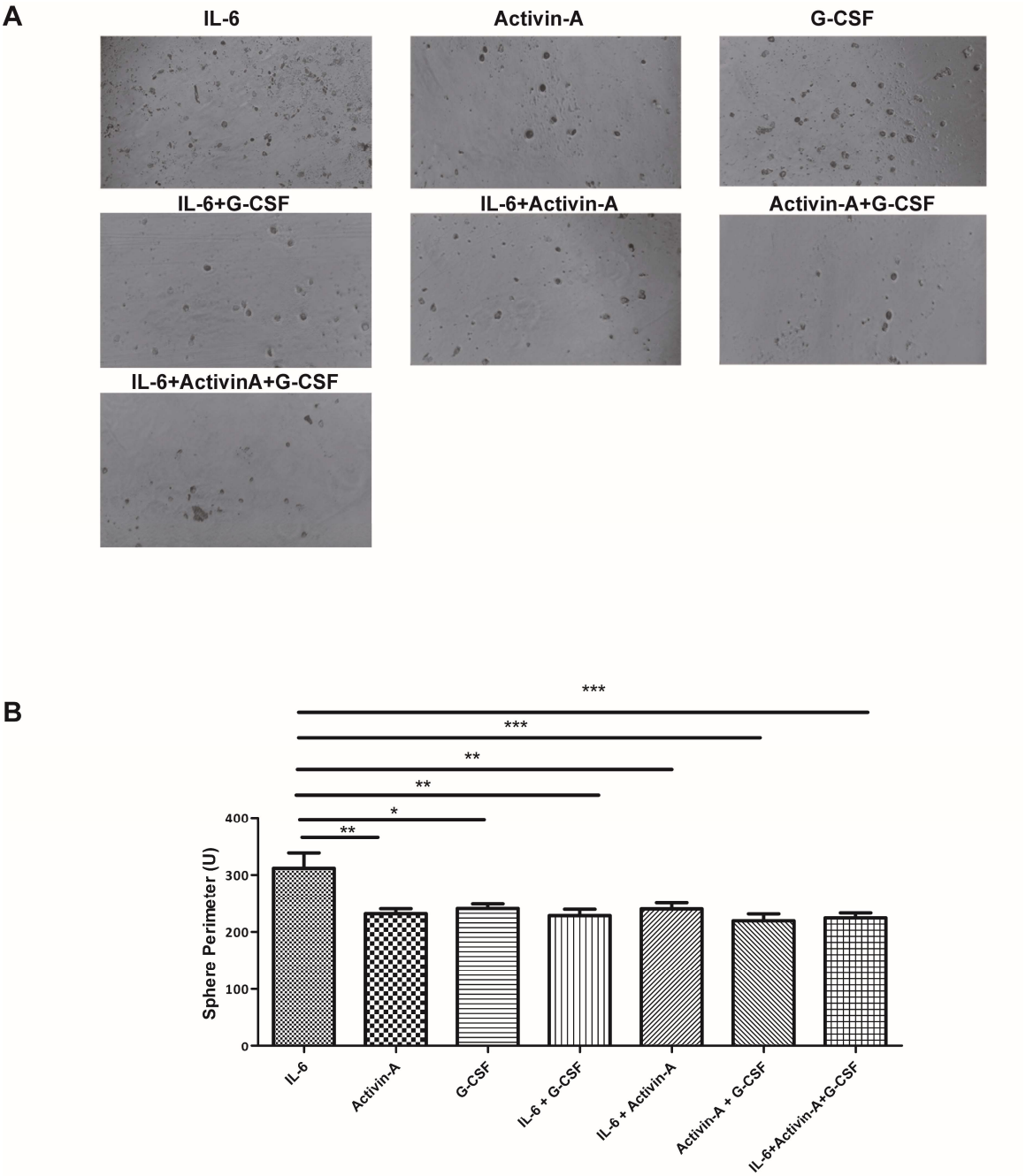

Figure S2 – Proof-of-concept experiment illustrating cytokines-mediated dedifferentiation. **(A)** SFA performed in different conditions of cytokines' abrogation, showing that spheres were observed whenever either IL-6 or Activin-A was present. G-CSF was unable to induce sphere formation. **(B)** Perimeter analysis. Corroborating the previous results, bigger spheres were attained when only IL-6 was present. A magnification of 100x was used in all panels. 10 spheres were measured in each condition. Data represent means ±SEM. Differences between the means were evaluated by one-way ANOVA followed by a Bonferroni post test.

References

1. Prasetyanti PR & Medema JP (2017) Intra-tumor heterogeneity from a cancer stem cell perspective. *Mol Cancer* 16(1):41.

2. Garvalov BK & Acker T (2011) Cancer stem cells: a new framework for the design of tumor therapies. *J Mol Med (Berl)* 89(2):95-107.

3. Li L & Neaves WB (2006) Normal stem cells and cancer stem cells: the niche matters. *Cancer Res* 66(9):4553-4557.

4. Qureshi-Baig K, Ullmann P, Haan S, & Letellier E (2017) Tumor-Initiating Cells: a criTICal review of isolation approaches and new challenges in targeting strategies. *Mol Cancer* 16(1):40.

5. Visvader JE (2011) Cells of origin in cancer. *Nature* 469(7330):314-322.

6. Medema JP (2013) Cancer stem cells: The challenges ahead. *Nat Cell Biol* 15(4):338-344.

7. Vermeulen L*, et al.* (2010) Wnt activity defines colon cancer stem cells and is regulated by the microenvironment. *Nat Cell Biol* 12(5):468-476.

8. Mani SA*, et al.* (2008) The Epithelial-Mesenchymal Transition Generates Cells with Properties of Stem Cells. *Cell* 133(4):704-715.

9. Chen X, Liao R, Li D, & Sun J (2016) Induced cancer stem cells generated by radiochemotherapy and their therapeutic implications. *Oncotarget* 8:17301-17312.

10. Rodrigues CFD*, et al.* (2009) Human bronchial epithelial cells malignantly transformed by hexavalent chromium exhibit an aneuploid phenotype but no microsatellite instability. *Mut Rese/Fundamental and Molecular Mechanisms of Mutagenesis* 670(1–2):42-52.

11. van Meerloo J, Kaspers GJL, & Cloos J (2011) Cell Sensitivity Assays: The MTT Assay. *Cancer Cell Culture: Methods and Protocols*, ed Cree IA (Humana Press, Totowa, NJ), pp 237-245.

12. V R (2006) Doubling Time Computing. *Available from: http://www.doubling-time.com/compute.php*

13. Franken NAP, Rodermond HM, Stap J, Haveman J, & van Bree C (2006) Clonogenic assay of cells in vitro. *Nat. Protoc* 1(5):2315-2319.

14. Raposo G*, et al.* (1996) B lymphocytes secrete antigen-presenting vesicles. *J Exp Med* 183(3):1161-1172.

15. Théry C, Amigorena S, Raposo G, & Clayton A (2006) Isolation and Characterization of Exosomes from Cell Culture Supernatants and Biological Fluids. *Curr Protoc Cell Biol*, (John Wiley & Sons, Inc.).

16. Subra C*, et al.* (2010) Exosomes account for vesicle-mediated transcellular transport of activatable phospholipases and prostaglandins. *J Lipid Res* 51(8):2105-2120.

17. Costa AN, Moreno V, Prieto MJ, Urbano AM, & Alpoim MC (2010) Induction of morphological changes in BEAS-2B human bronchial epithelial cells following chronic sub-cytotoxic and mildly cytotoxic hexavalent chromium exposures. *Mol Carcinog* 49(6):582-591.

18. Flaveny CA*, et al.* (2015) Broad Anti-tumor Activity of a Small Molecule that Selectively Targets the Warburg Effect and Lipogenesis. *Cancer Cell* 28(1):42-56.

19. Martins-Neves SR*, et al.* (2012) Therapeutic implications of an enriched cancer stem-like cell population in a human osteosarcoma cell line. *BMC Cancer* 12:139-139.

20. Liberti MV & Locasale JW (2016) The Warburg Effect: How Does it Benefit Cancer Cells? *Trends Biochem Sci* 41(3):211-218.

21. Vermeulen L, Sprick MR, Kemper K, Stassi G, & Medema JP (2008) Cancer stem cells - old concepts, new insights. *Cell Death Differ* 15(6):947-958.

22. Pradella D, Naro C, Sette C, & Ghigna C (2017) EMT and stemness: flexible processes tuned by alternative splicing in development and cancer progression. *Mol Cancer* 16(1):8.

23. Kalluri R & Weinberg RA (2009) The basics of epithelial-mesenchymal transition. *J Clin Invest* 119(6):1420-1428.

24. Mendez MG, Kojima S, & Goldman RD (2010) Vimentin induces changes in cell shape, motility, and adhesion during the epithelial to mesenchymal transition. *FASEB J* 24(6):1838-1851.

25. Barr MP*, et al.* (2013) Generation and characterisation of cisplatin-resistant non-small cell lung cancer cell lines displaying a stem-like signature. *PLoS One* 8(1):e54193.

26. Gupta PB*, et al.* (2009) Identification of selective inhibitors of cancer stem cells by high-throughput screening. *Cell* 138(4):645-659.

27. Lee HE*, et al.* (2011) An increase in cancer stem cell population after primary systemic therapy is a poor prognostic factor in breast cancer. *Br J Cancer* 104(11):1730-1738.

28. Liu H, Lv L, & Yang K (2015) Chemotherapy targeting cancer stem cells. *Am J Cancer Res* 5(3):880-893.

29. Blanpain C (2013) Tracing the cellular origin of cancer. *Nat Cell Biol* 15(2):126-134.

30. Gottschling S, Schnabel PA, Herth FJF, & Herpel E (2012) Are we Missing the Target? – Cancer Stem Cells and Drug Resistance in Non-small Cell Lung Cancer. *Cancer Genomics - Proteomics* 9(5):275-286.

31. Wilson BJ*, et al.* (2011) ABCB5 Identifies a Therapy-Refractory Tumor Cell Population in Colorectal Cancer Patients. *Cancer Res* 71(15):5307-5316.

32. Bang C & Thum T (2012) Exosomes: New players in cell–cell communication. *The Int J Biochem Cell Biol* 44(11):2060-2064.

33. Thery C, Ostrowski M, & Segura E (2009) Membrane vesicles as conveyors of immune responses. *Nat Rev Immunol* 9(8):581-593.

34. Christianson HC, Svensson KJ, van Kuppevelt TH, Li JP, & Belting M (2013) Cancer cell exosomes depend on cell-surface heparan sulfate proteoglycans for their internalization and functional activity. *Proc Natl Acad Sci U S A* 110(43):17380-17385.

35. Duelen R*, et al.* (2017) Activin A Modulates CRIPTO-1/HNF4alpha+ Cells to Guide Cardiac Differentiation from Human Embryonic Stem Cells. *Stem Cells Int* 2017:4651238.

36. Merfeld-Clauss S, Lease BR, Lu H, March KL, & Traktuev DO (2016) Adipose stromal cells differentiation toward smooth muscle cell phenotype diminishes their vasculogenic activity due to induction of activin A secretion. *J Tissue Eng Regen Med*:n/a-n/a.

37. Rolletschek A, Kania G, & Wobus AM (2006) Generation of pancreatic insulin-producing cells from embryonic stem cells — 'Proof of principle', but questions still unanswered. *Diabetologia* 49(11):2541-2545.

38. Zhu L*, et al.* (2016) Crosstalk between bone marrow-derived myofibroblasts and gastric cancer cells regulates cancer stemness and promotes tumorigenesis. *Oncogene* 35(41):5388-5399.

39. Sansone P*, et al.* (2016) Self-renewal of CD133(hi) cells by IL6/Notch3 signalling regulates endocrine resistance in metastatic breast cancer. *Nat Commun* 7:10442.

40. Cortini M, Massa A, Avnet S, Bonuccelli G, & Baldini N (2016) Tumor-Activated Mesenchymal Stromal Cells Promote Osteosarcoma Stemness and Migratory Potential via IL-6 Secretion. *PLoS One* 11(11):e0166500.

41. Lambert AW, *et al.* (2016) Tumor Cell-Derived Periostin Regulates Cytokines That Maintain Breast Cancer Stem Cells. *Mol Cancer Res* 14(1):103-113.

42. Agarwal S, *et al.* (2015) G-CSF Promotes Neuroblastoma Tumorigenicity and Metastasis via STAT3-Dependent Cancer Stem Cell Activation. *Cancer Res* 75(12):2566-2579.